

Dense bubble flow in a silo: an unusual flow of dispersed medium

Yann Bertho, Christophe Becco, and Nicolas Vandewalle
 Group for Research and Applications in Statistical Physics (GRASP),
 Institut de Physique B5a, Université de Liège, 4000 Liège, BELGIUM

The dense flow of air bubbles in a two-dimensional silo (through an aperture D) filled with a liquid is studied experimentally. A particle tracking technique has been used to bring out the main properties of the flow: displacements of the bubbles, transverse and axial velocities. The behavior of the air bubbles is observed to present similarities with non-deformable solid grains in a granular flow. Nevertheless, a correlation between the bubble velocities and their deformations has been evidenced. Moreover, a new discharge law (Beverloo-like) must be considered for such a system, where the flow rate is observed to vary as $D^{1/2}$ and depends on the deformability of the particles.

PACS numbers: 47.50.+d, 47.60.+i, 82.70.-y, 83.50.-v, 83.80.-k

Structured fluids like granular materials or aqueous foams received much attention from physicists during the last decade. Indeed, they are ubiquitous in nature and in industrial processes [1, 2], and exhibit striking rheological behaviors as compared to conventional liquids. These materials involve multiple physical processes and cooperative phenomena such as shear banding, inter-particles interactions and the formation of ‘arches’ redirecting the forces inside the material [3, 4]. Such processes are then able to provoke intermittent flows [5] or jamming [6] because of the topological constraints that develop since the particles (grains or bubbles) press against each other. This contributes to the complex flow behavior of granular media and foams.

The present study deals with bubble assemblies where the bubbles are predominantly spherical so that the contacts between two adjacent bubbles are reduced. The liquid fraction in the material is high enough to consider the diffusion of air through the bubble boundaries as negligible at the time scale of the experiments.

Bubble assemblies can also be seen as a granular medium where contacting particles are characterized by a nearly zero friction. Thus, we have a remarkable system with a low energy dissipation at the contacts in comparison with traditional grain assemblies. Even if bubble flows present strong analogies with granular flows, we must keep in mind that the nature of the interactions between the particles is totally different. Moreover, in contrast with granular materials, the bubbles may undergo strong deformations when they are subjected to a constraint. Some works are focused on the velocity profiles [7], the rearrangements [8] and deformations [9] in slowly sheared bubble rafts. Our interest is to compare rapid flows of bubbles and granular media to identify the main physical properties in such dispersed media.

In this paper, the flow of a two-dimensional (2D) foam is analyzed experimentally [10, 11]. The setup consists of a transparent inclined glass plane of width $W = 130\text{ mm}$ which is immersed into water (Fig. 1). The tilt angle θ of the plane can be adjusted by a fine screwing system. Spherical quasi-monodisperse

air bubbles are then injected at the bottom of the inclined plane by blowing air through a needle (the height h of the piling is kept roughly constant during the experiments $h \simeq 200\text{ mm}$). Note that the tilt angle is small (θ ranges from 0° to 1°) to ensure that only one layer of bubbles is created in the perpendicular direction to the plane and to decrease the influence of the gravity (*i.e.* drainage). Bubble size is controlled by an air pump and is kept roughly constant in the present study [diameter $d = (5.4 \pm 0.3)\text{ mm}$]. In order to avoid the coalescence of the bubbles, dish-washing liquid is mixed into water. Due to buoyancy, the bubbles rise underneath the inclined plane and tend to pack on a transverse wall placed at the top of the plane. An orifice of width D at the center (x_0, y_0) of this obstacle allows the bubbles to empty out the silo. Our experiment is then analogous to the gravity-driven granular flow in a flat bottomed 2D silo, emptying out of a central orifice [12]. Top views of the bubble packing are recorded through the transparent tilted plane by means of a CCD camera at a frame rate of 50 frames per second. In order to quantify and to measure the main properties

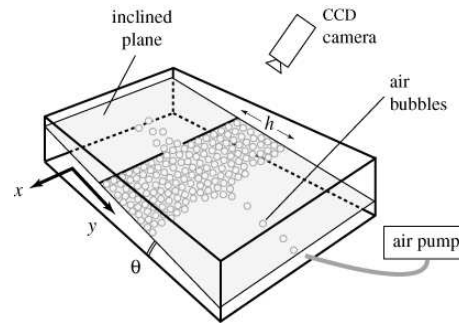


FIG. 1: Sketch of the experimental setup. A transparent inclined plane is immersed into water and tilted at an angle θ . Small air bubbles are injected from below at the bottom of the plane and rise towards the top where they aggregate. Motions of the bubbles are recorded by a CCD camera.

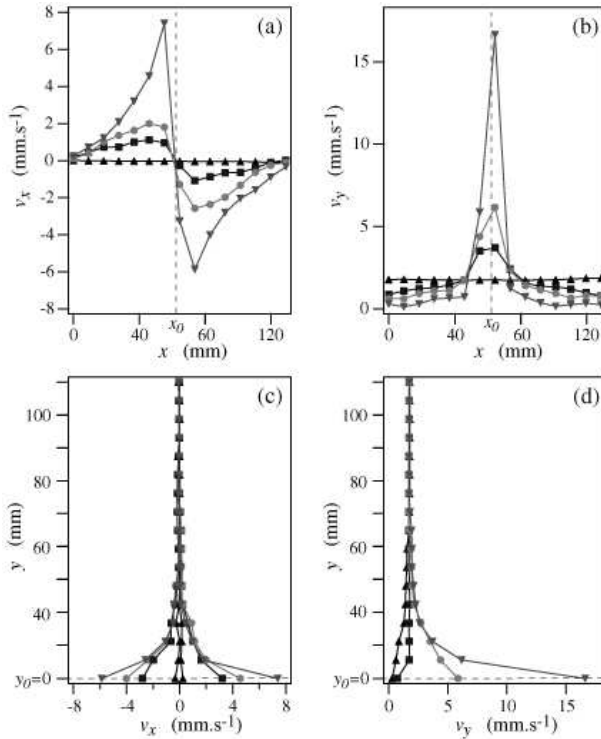


FIG. 2: Transverse v_x and longitudinal v_y velocity profiles during the discharge of a silo ($\theta \simeq 0.63^\circ$, $D \simeq 8.6$ mm). (—) position (x_0, y_0) of the center of the outlet of the silo. The different curves (\blacktriangledown , \bullet , \blacksquare , \blacktriangle) correspond respectively to velocity profiles at increasing distances from $y_0 = 0$ (Figs. 2a and 2b) and increasing distances from x_0 (Figs. 2c and 2d).

of the flow, the motion of each bubble in the packing (≈ 2000 bubbles per frame) has been tracked through image analysis.

Figure 2 displays typical transverse v_x and longitudinal v_y velocities of the bubbles as a function of x and y at different height in the packing. In the top part of the silo [(\blacktriangle) in Fig. 2b], a block motion is observed: the longitudinal velocity v_y remains constant reflecting low interactions between the bubbles and the side walls (slipping motion). As y decreases (*i.e.* the bubbles move towards the outlet), the flow takes place in a triangular-shaped domain where the fastest bubbles are located in the center of the silo and the slowest or motionless ones at the walls [(\blacktriangledown) in Fig. 2b]. This is in agreement with the ‘V-shape’ of mobile grains observed during the flow of granular materials in silos or hourglasses [12, 13]. Far from the outlet ($y \gtrsim 15d$), bubbles have a nearly zero transverse velocity (Fig. 2c) and a constant longitudinal velocity v_y (Fig. 2d). For lower values of y , the velocity distribution of the bubbles deep inside the silo is totally modified: a transverse component of velocity v_x appears in the flow conducting the bubbles towards the orifice while v_y increases strongly near the outlet.

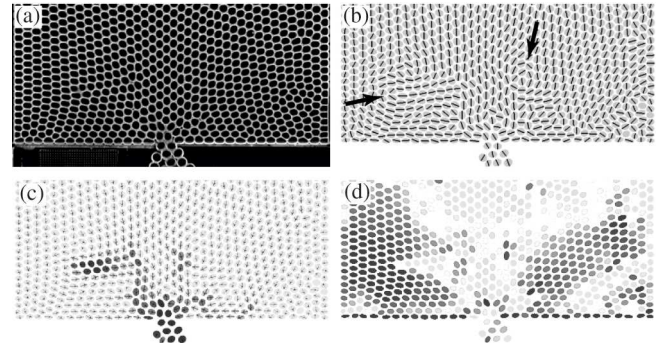


FIG. 3: Typical recordings of the bubble discharge: (a) snapshot of the experimental flow, (b) displacement field, (c) velocity field (the fastest bubbles appear darker), (d) deformation field (the more constrained bubbles appear darker). Arrows in Fig. 3b point out a dislocation and a recirculation zone.

A zoom of the bottom part of the silo of height 60 mm is shown in Fig. 3a. Image analysis allows one to extract the position of each bubble in the stack and evaluate the displacement profile (Fig. 3b) and the velocity field (Fig. 3c) during the flow. Figure 3d displays the deformation field and provides information concerning the constraints undergone inside the dense bubble assembly.

In contrast with granular materials where the flow occurs only in a cone-shaped central region of the silo (while the grains located in the regions near the side walls are motionless) [12, 13], note that motions of bubbles are detected everywhere in the silo. Moreover, the bubble tracking put into evidence recirculation zones and the propagation of dislocations (shear bands) during the bubble flow. As expected in two-dimensional nearly monodisperse flows, bubbles tend to pack in an ordered hexagonal structure at the top of the bubble packing (Fig. 3a); these organized domains are separated by the dislocations. Motions of blocks of bubbles are observed and look like crystal domains. Those blocks are sliced by fast-moving defects along bubble lines. The movement is not simultaneous along the whole row but begins at one end with the appearance of a dislocation running along the slip line. This process is initiated at the orifice of the silo and propagates towards the bulk after many rebounds on the side walls. Both recirculation zone and dislocation appear clearly as pointed out by the arrows in Fig. 3b.

The velocity $v = (v_x^2 + v_y^2)^{1/2}$ of each bubble has been computed and superimposed on the images of the flow (the darkest bubbles corresponding to the fastest ones). The recirculation regions and the dislocation observed in Fig. 3b are characterized by a mean velocity higher than in the rest of the silo (Fig. 3c).

The deformation of a bubble is evaluated by fitting the bubble shape by an ellipse and computing its eccentricity [14]. As pointed out in Fig. 3d, the fastest

bubbles are observed to correspond to the less deformed ones. Moving bubbles press against surrounding ones and to deform them. This is especially the case near the dislocation. Therefore, in such dense bubble flows, spherical bubbles are located far from the outlet and propagate in a block motion at a constant velocity or in the dislocation, while flattest ones correspond to crushed bubbles against the bottom wall or constraint bubbles inside the pile.

A classic paper on the flow of granular solids through orifices is that of Beverloo *et al.* [15]. Using a straightforward dimensional analysis, they pointed out that the grain flow rate Q_g is a power law in D (where D is the diameter of the orifice). The power depends on the dimensionality of the flow [13, 15, 16], so that for a 2D flow $Q_g \propto g^{1/2} D^{3/2}$. A corrective term is usually added to take into account the mean diameter of the grains d_g :

$$Q_g \propto g^{1/2} (D - kd_g)^{3/2}, \quad (1)$$

where k is an empirical constant depending on the particle shape and the grain interactions ($k \simeq 1.5$ for beads).

The bubble flow rate Q has been evaluated by counting the number of bubbles flowing out of the silo, at different tilt angles θ of the plane. Figure 4a shows that Q varies as $(\sin \theta)^{3/2}$. The behavior of bubble flow through an aperture is thus drastically different from the one of a granular flow for which Q_g varies as $g^{1/2}$. This is probably due to the nature of forces between the particles and with the walls: the frictions inside a granular medium are much more important than in a bubble flow and consequently slow down the silo discharge.

Figure 4b displays the bubble flow rate Q as a function of the normalized aperture of the silo D/d . In contrast with granular materials for which the flow rate Q_g vanishes for $D/d \lesssim 1.5$ due to the formation of arches [Eq. (1)], Q is observed to be non-zero for smaller values of the aperture. Bubbles can pass through an aperture of the order of $2d/3$ after having undergone strong shape deformations. The value of $k \simeq 2/3$ should then depend mainly on the bubble size and the surface tension of the liquid; these assumptions will receive special care in a subsequent work. Moreover, note that Q varies as $(D/d)^{1/2}$ which is significantly different from the case of a 2D granular material flowing down a silo where the power is $3/2$.

Following a similar approach suggested by Bazant [17] to describe grain flows in silos, we propose that sets of bubbles undergo cooperative displacements and move as blocks during the emptying. This is clearly the case in the upper part of the silo where a block motion is observed (see the bubble velocity (\blacktriangle) in Fig. 2b) and in agreement with direct observations near the outlet where domains are separated by dislocations (Fig. 3). Considering a typical size L for the flowing sets of bubbles in a

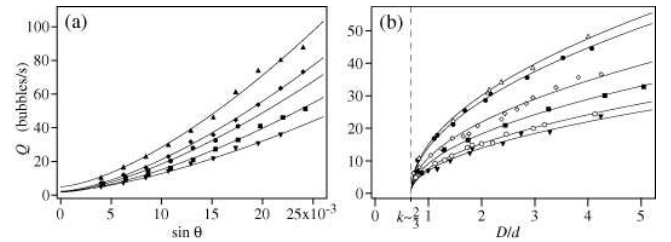


FIG. 4: Bubble flow rate Q as a function of:

(a) the tilt angle θ for different apertures D of the silo: (\blacktriangledown) $D = 6.3$ mm, (\blacksquare) $D = 8.0$ mm, (\bullet) $D = 9.7$ mm, (\blacklozenge) $D = 12.8$ mm, (\blacktriangle) $D = 19.9$ mm; (—) best fits of the experimental data with $Q \propto (\sin \theta)^{3/2}$.

(b) the normalized aperture D/d of the silo for different tilt angles θ : (\blacktriangledown) $\theta = 0.46^\circ$, (\circ) $\theta = 0.50^\circ$, (\blacksquare) $\theta = 0.56^\circ$, (\diamond) $\theta = 0.63^\circ$, (\bullet) $\theta = 0.75^\circ$, (\triangle) $\theta = 0.82^\circ$; (—) best fits of the experimental data with $Q \propto (D/d - k)^{1/2}$, with $k \simeq \frac{2}{3}$.

cooperative motion, one should note that their motion is mainly limited by the viscous drag force f , proportional to

$$f \propto \eta Lv, \quad (2)$$

where v is the terminal velocity of the bubble set in a fluid of viscosity η . Moreover, the bubbles at the outlet of the silo (aperture D) are affected by the buoyancy B coming from the bubbles located behind them, so that

$$B = \frac{2}{3} \phi h D d \Delta \rho g \sin \theta, \quad (3)$$

where $\Delta \rho$ is the difference between liquid and air densities and h the height of the bubble packing. This assumes that, in a first approximation, no arch is created in the bubble packing so that the force transmission remains essentially in the y -direction of the mean flow. Thus, the buoyancy felt at the outlet comes mainly from bubbles located in a region $(D \times h)$ upstream from the aperture. ϕ represents the mean bubble fraction in the stack and holds information both on the organization of the bubble lattice (ϕ decreases as the material goes away from the dense ordered triangular packing) and on the capability of the bubbles to warp their shape (ϕ increases for compressed and deformed bubbles). The equilibrium between the buoyancy and the drag force leads then to a terminal velocity v proportional to:

$$v \propto \frac{\phi h D d}{\eta L} \Delta \rho g \sin \theta. \quad (4)$$

The number of bubble blocks in the silo is directly related to the number n of defects created at the outlet and giving birth to dislocations in the stack; in other words, n bubble sets of typical size L are created in a region D^2 near the outlet, hence $nL^2 \simeq D^2$. Moreover, the number n of defects at the outlet varies as D/d : the larger the

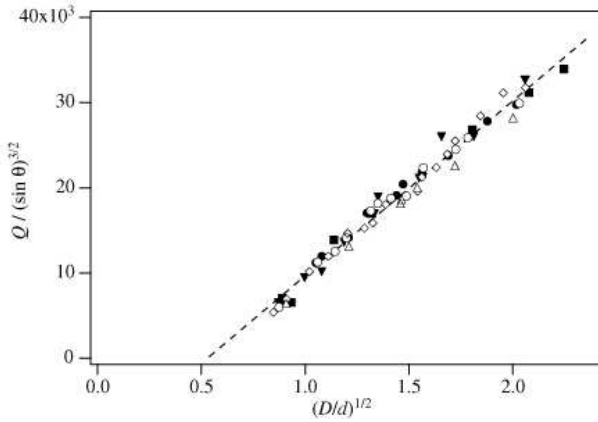


FIG. 5: Rescaling of all measurements using Eq. (8) for (\blacktriangledown) $\theta = 0.46^\circ$, (\circ) $\theta = 0.50^\circ$, (\blacksquare) $\theta = 0.56^\circ$, (\diamond) $\theta = 0.63^\circ$, (\bullet) $\theta = 0.75^\circ$, (\triangle) $\theta = 0.82^\circ$.

aperture D of the silo, the more the number of created defects. Hence, the number of dislocations generated at the outlet increases with D , separating the bubble medium in more, and consequently smaller, domains of typical size L . Hence, one can write

$$L \propto D \left(\frac{d}{D} \right)^{1/2}. \quad (5)$$

Dimensionally, the bubble flow rate Q can be written as the quotient of a characteristic velocity v and a characteristic length l . The flow of air bubbles in a liquid being strongly governed by the surface tension γ of the liquid, a natural characteristic length l is then an effective capillary length, defined as

$$l = \sqrt{\frac{\gamma}{\Delta \rho g \sin \theta}}. \quad (6)$$

As a result, combining Eqs. (4) and (6), and using the expression of L given by Eq. (5), the bubble flow rate Q can be written as follow:

$$Q \propto \frac{\phi h}{\eta \gamma^{1/2}} \left(\frac{D}{d} \right)^{1/2} (\Delta \rho g \sin \theta)^{3/2}, \quad (7)$$

which agrees with behaviors emphasized in Fig. 4. The bubble flow rate is then observed to decrease when the viscosity η of the fluid is increased. Moreover, the lower the surface tension γ , the more the bubbles are able to change their shape, making easier the discharge. At the opposite, increasing γ reduces the capacity of deformation of the bubbles: the material becomes more rigid and tends to be more similar to a traditional granular material where formation of arches are observed at the outlet, leading to the blockage of the flow. Finally, one will note that increasing the height h of the bubble packing contributes to an increase of the buoyancy felt at the outlet, and consequently to an increase of the bubble flow rate.

These results enhance the fact that a new Beverloo's law must be considered in the particular case of bubble flows and more generally concerning the flow of deformable dispersed media. Figure 5 displays a rescaling of all measurements and confirms that the Beverloo's law for a deformable dispersed medium is given by

$$Q \propto (g \sin \theta)^{3/2} \left(\frac{D}{d} - k \right)^{1/2}, \quad (8)$$

where k is related to the deformation capability of the particles.

In summary, the present experiment shows that velocity profiles in a bubble flow in silo present strong similarities with a granular flow but with sliding motions at the walls. A correlation between the velocity and the deformation of the bubbles has been observed. Moreover, we demonstrate that a new Beverloo's law [Eq. (8)] must be considered for the specific case of deformable dispersed media flowing out a silo, where the flow rate varies as $D^{1/2}$ and depends on the nature of the particles and more precisely of their capability to deform themselves.

The authors thank H. Caps, S. Dobolo, F. Ludewig and G. Lumay for helpful discussions during this work. Y. B. benefits from a postdoctoral fellowship supported by the ARC programme number 02/07-293.

-
- [1] J. Duran, *Sands, powders and grains* (Springer-Verlag, 2000).
 - [2] D. Weaire and S. Hutzler, *The physics of foams* (Oxford Univ. Press, 1999).
 - [3] H. A. Janssen, Z. Ver. Dtsch. Ing. **39**, 1045 (1895).
 - [4] Y. Bertho and F. Giorgiutti-Dauphiné and J. -P. Hulin, Phys. Rev. Lett. **90**, 144301 (2003).
 - [5] Y. Bertho and F. Giorgiutti-Dauphiné and J. -P. Hulin, Phys. Fluids **15**, 3358 (2003).
 - [6] S. Rodts and J. C. Baudez and Ph. Coussot, Europhys. Lett. **69**, 636 (2005).
 - [7] J. Lauridsen and G. Chanan and M. Dennin, Phys. Rev. Lett. **93**, 018303 (2004).
 - [8] M. Dennin, Phys. Rev. E **70**, 041406 (2004).
 - [9] E. Janiaud and F. Graner, J. Fluid Mech. **532**, 243 (2005).
 - [10] W. L. Bragg and J. F. Nye, Proc. R. Soc. London **190**, 474 (1947).
 - [11] N. Vandewalle and S. Trabelsi and H. Caps, Europhys. Lett. **65**, 316 (2004).
 - [12] A. Medina and J. Andrade and C. Trevino, Phys. Lett. A **249**, 63 (1998).
 - [13] D. Hirshfeld and Y. Radzyner and D. C. Rapaport, Phys. Rev. E **56**, 4404 (1997).
 - [14] C. Ybert and J.-M. di Meglio, C. R. Physique **3**, 555 (2002).
 - [15] W. A. Beverloo and H. A. Leniger and J. Van De Velde, Chem. Eng. Sci. **15**, 260 (1961).
 - [16] A. A. Mills and S. Day and S. Parkes, Eur. J. Phys. **17**, 97 (1996).
 - [17] M. Z. Bazant, cond-mat/0307379 v2.